World Academy of Science, Engineering and Technology
International Journal of Electronics and Communication Engineering
Vol:2, No:5, 2008

Sensor Optimisation via H_∞ Applied to a MAGLEV Suspension System

Konstantinos Michail, Argyrios Zolotas, Roger Goodall, and John Pearson

***Abstract*—**In this paper a systematic method via H_∞ control design is proposed to select a sensor set that satisfies a number of input criteria for a MAGLEV suspension system. The proposed method recovers a number of optimised controllers for each possible sensor set that satisfies the performance and constraint criteria using evolutionary algorithms.

***Keywords*—**H-infinity, Sensor optimisation, Genetic algorithms, MAGLEV vehicles

I. INTRODUCTION

A sensor optimisation systematic framework is considered for a MAGnetic LEVitated (MAGLEV) transport vehicle [11]. This work is part of a bigger project investigating optimised configurations of sensing elements for control and fault tolerant. The research is focusing upon practical engineering applications that are dynamically complex, electromechanical in nature and typified the kinds of systems in aerospace, automotive and railway. The model considered is a linearised electromagnetic suspension system of a quarter car in state space form with five possible measurements leading to $2^5 - 1 = 31$ possible sensor combinations. The framework presented aims to find a set of optimised controllers that improve the ride quality while minimizing the control effort and the performance metric within a range of hard and soft constraints assigned beforehand for each sensor combination. Both deterministic and stochastic track disturbances are considered, with noise and noise-free measurement conditions.

This framework merges the H_∞ controller design, the Linear Matrix Inequalities (LMI) optimisation tool and heuristic algorithms that are used to adjust the H_∞ weighting filters and achieve a Pareto front of optimised controllers solution for each sensor set. Among the metaheuristic algorithms [5], the evolutionary algorithms are used extensively in engineering and are being proved to perform satisfactorily for hard engineering optimisation problems [6]. Note that a scheme of loop-shaping design procedure (LSDP) on a MAGLEV suspension application was presented in [2] using genetic algorithms but on the control design rather than the optimisation of sensor configurations.

The **N**on-dominated **S**orting **G**enetic **A**lgorithms II (**NSGAII**) method introduced in [4], proves to be a power optimisation tool, and is the class of evolutionary algorithms implemented in the proposed framework.

Authors are with Control Systems Group, Department of Electronic and Electrical Engineering, Loughborough University, UK. emails: {k.michail, a.c.zolotas, r.m.goodall, j.t.pearson}@lboro.ac.uk. This work was supported in part under the EPSRC (UK) project Grant Ref. EP/D063965/1 and BAE Systems (SEIC),UK.

This paper is organised as follows: Section two discuss the linearised model of a MAGLEV suspension and the possible input disturbances to the system. Section three presents the requirements of the MAGLEV suspension as well as the objective functions to be minimised, the overall problem formulation, and the genetic algorithm parameter adjustment. Moreover presents how the constraints are merged into the algorithm procedure. Simulations and data analysis of the overall framework are given in section 4 with a comparison between noisy and noise-free measurements. Conclusions with future work are given in section 5.

II. MODEL DESCRIPTION

The diagram of a one degree-of-freedom, 'quarter-car' electromagnetic suspension system is shown in Fig.1. The suspension consists of an electromagnet with a ferromagnetic core and a coil of N turns which is attracted to the rail that is made out of ferromagnetic material. The carriage mass is attached on the electromagnet, with z_t being the rail position and z the electromagnet position. The air gap $(z_t - z)$ is to be maintained close to the operating condition required. The

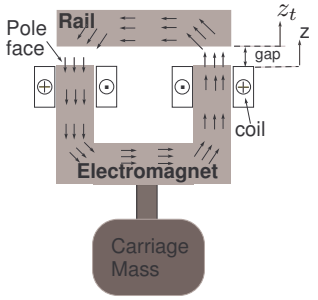

Fig. 1. Suspension system for MAGLEV

LTI state space model is derived by considering the operating point (nominal) values of the coil current I_0, flux B_0, force F_0 and air gap G_0. The following relationships hold

$$F = f + F_0, \qquad B = b + B_0$$
$$G = (z_t - z) + G_0, \quad I = i + I_0 \tag{1}$$

where, $f, b, (z_t - z)$ and i are small variations around their nominal values. The fundamental magnetic relationships are $F \propto B^2$ and $B \propto I/G$, thus, the linearised expressions for the magnet are [9]

$$b = K_i i - K_{(z_t - z)}(z_t - z) \tag{2}$$
$$f = K_b b \tag{3}$$

where $K_i = B_0/I_0$, $K_{(z_t-z)} = B_0/G_0$ and $K_b = 2F_0/B_0$. The voltage v, applied to the coil is given by:

$$v = Ri + L\frac{di}{dt} + NA\frac{db}{dt} \tag{4}$$

where N is the number of coil turns, R the coil resistance, A is the pole face area and L the coil inductance. Moreover, the force f depends on the mass M and the vertical acceleration $\ddot{z}$.

$$f = M\ddot{z} \quad and \quad f = K_b b \tag{5}$$

therefore, from (5) and (2) the equation for $\ddot{z}$ is

$$\ddot{z} = \frac{K_b K_i}{M} i - \frac{K_b K_{(z_t-z)}}{M}(z_t - z) \tag{6}$$

where $(z_t - z)$ is the air gap between the rail and the electromagnet. Also, from (2) and (6) the current equation is

$$\frac{di}{dt} = \frac{V}{L + NAK_i} + \frac{NAK_{(z_t-z)}}{L + NAK_i}(\dot{z}_t - \dot{z}) - \frac{Ri}{L + NAK_i} \tag{7}$$

and from (6) and (7) a state vector can be constructed as follows

$$X = \begin{bmatrix} i & \dot{z} & (z_t - z) \end{bmatrix}^T \tag{8}$$

with the relevant state space expression given by

$$\dot{X} = A_g X + B_v v + B_z \dot{z}_t, \quad y = CX \tag{9}$$

where matrices

$$A_g = \begin{pmatrix} -\frac{R}{L+K_i NA} & -\frac{K_{(z_t-z)}NA}{L+K_i NA} & 0 \\ \frac{K_b K_i}{M} & 0 & -\frac{K_b K_{(z_t-z)}}{M} \\ 0 & -1 & 0 \end{pmatrix} \tag{10}$$

$$(B_v \;\; B_z) = \begin{pmatrix} \frac{1}{L+K_i NA} & \frac{K_{(z_t-z)}NA}{L+NAK_i} \\ 0 & 0 \\ 0 & 1 \end{pmatrix} \tag{11}$$

$$C = \begin{pmatrix} 1 & 0 & 0 \\ K_i & 0 & -K_{(z_t-z)} \\ 0 & 0 & 1 \\ 0 & 1 & 0 \\ \frac{K_b K_i}{M} & 0 & -\frac{K_b K_{(z_t-z)}}{M} \end{pmatrix} \tag{12}$$

Note that the output matrix in (12) refers to all possible measurements that can be considered ($y = [i\ b\ (z_t - z)\ \dot{z}\ \ddot{z}]^T$). The parameter values for a one tone suspension system are shown in Table I. Note that the maglev system is open-loop unstable.

TABLE I
PARAMETERS OF MAGNETIC SUSPENSION

$M = 1000kg$	$R = 10\Omega$	$I_0 = 10A$
$G_0 = 0.015m$	$L = 0.1H$	$A = 0.01m^2$
$B_0 = 1T$	$N = 2000$	$F_0 = 10000N$

A. Rail disturbances to the suspension

Two track input characteristics are considered, i.e. deterministic changes such as gradients or curves and stochastic (random) changes in the track position due to misalignments.

1) Random input: Random behavior of the rail position is caused as the vehicle moves along by track-laying inaccuracies and steel rail discrepancies. Consider the vertical direction, the velocity variations are quantified by a double-sided power spectrum density (PSD) which in the frequency domain is expressed by

$$S_{\dot{z}_t} = \pi A_r V \tag{13}$$

where, V is the vehicle speed (in this work is taken as $15m/s$) and A_r represents the track roughness equal to $1 \times 10^{-7} m$ (for a typical high quality track). The corresponding (one-sided) autocorrelation function is given by

$$R(\tau) = 2\pi^2 A_r V \delta(\tau) \tag{14}$$

2) Deterministic input: The main deterministic inputs to a suspension for the vertical direction are transitions onto gradients. In this work, the deterministic input components utilised are shown in Fig.2 and represent a gradient of 5% at a vehicle speed of $15m/s$ and an allowed acceleration of $0.5m/s^2$.

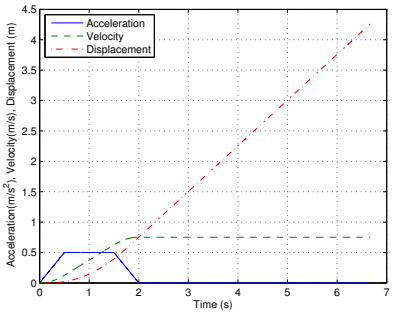

Fig. 2. Deterministic input to the suspension with a vehicle speed of $15ms^{-1}$ and 5% gradient.

III. PROBLEM FORMULATION

A. Design requirements

Fundamentally there is a trade off between the deterministic and the stochastic response (ride quality) of the suspension. For slow speed vehicles, performance requirements are described in [7] and [8]. In particular, the practical objective is to minimize both the vertical acceleration (improve ride quality) and the RMS current variations. The H_∞ performance (γ_{opt}) measure has also been assigned as an additional objective. These objectives can be can be formally written as

$$\phi_1 = i_{rms}, \quad \phi_2 = \ddot{z}_{rms}, \quad \phi_3 = \gamma_{opt} \tag{15}$$

with the constraints given in Table II. All constraints are soft constraints except the steady state error which is required to be zero and has been set as a hard constraint.

B. Sensor optimisation

The problem set up is shown in Fig. 3. The aim is to tune the weights (W_p, W_u) so that a set of optimised controllers $(\mathbf{K}(\mathbf{s}))$ are recovered that satisfy all of the constraints showed in

TABLE II
CONSTRAINTS FOR THE MAGNETIC SUSPENSION PERFORMANCE.

Constraints	Value
RMS acceleration($\simeq 5\%' g'$),($\ddot{z}_{rms}$)	$< 0.5ms^{-2}$
RMS air gap variation, $((z_t - z)_{rms})$	$< 5mm$
Maximum air gap deviation,$((z_t - z)_p)$	$< 7.5mm$
Control effort,(V_p)	$< 300V(3I_0R_0)$
Settling time, (t_s)	$< 3s$
Air gap Steady state error, $((z_t - z)_{e_{ss}})$	$= 0$

section III-A for each sensor set (y) that is available for measurement. Note that the sensor combinations are selected using the output matrix (C_y) as shown in equation (16). The total measurements available are 5 $(i, b, (z_t - z), \dot{z}_t, \ddot{z}_t)$ as described in section II resulting to 31 sensor sets $(i.e \quad i, b, i\dot{z}, b\ddot{z}...etc)$. The MAGLEV state equation in (9) is imposed into the

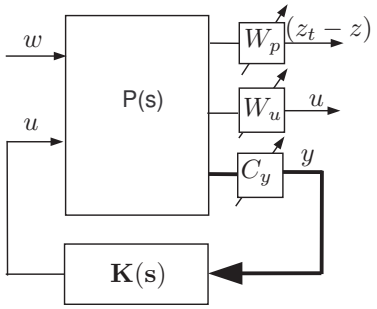

Fig. 3. Multi-objective generalised plant configuration.

generalised form of (16).

$$\begin{aligned} \dot{x} &= Ax + B_z w + B_u u \\ z_\infty &= C_\infty x + D_{\infty 1} w + D_{\infty 2} u \\ y &= C_y x + D_{y1} w + D_{y2} u \end{aligned} \tag{16}$$

w is exogenous inputs (as described in Section II-A), u the controller output, z_∞ is the regulated output, i.e control effort and air gap $(z_t - z)$ and y is the corresponding sensor set. The infinity norm of the closed loop transfer function from the exogenous inputs to the regulated outputs is minimized subject to the constraints mentioned in III-A.

$$\| T_{zw} \|_\infty < \gamma \tag{17}$$

This problem is solved for each sensor set, and for each random pair of weighting functions produced by the genetic algorithm, via LMI formulation (18). This can be easily solved in MATLAB using function *'hinfmix'* of the robust control toolbox.

$$\begin{bmatrix} A_{cl}x_\infty + x_\infty A_{cl}^T & B_{cl} & x_\infty C_{cl1}^T \\ B_{cl}^T & -I & D_{cl1}^T \\ C_{cl1}x_\infty & D_{cl1} & -\gamma^2 I \end{bmatrix} < 0 \tag{18}$$

subject to $x_\infty > 0$.

The weighting filters W_p and W_u are appropriate low pass and high pass filters respectively (see 19), to adjust the performance of the controller by varying their parameters. There is no general approach to select weighting functions as this depends on the application but some guidelines on selecting the weights for the H_∞ design of a plant are suggested in [12].

$$W_p = \left(\frac{\frac{s}{M_p^{1/n_p}} + \omega_b}{s + \omega_b A_p^{1/n_p}} \right)^{n_p} \qquad W_u = \left(\frac{\tau s + A_u^{1/n_u}}{\frac{\tau}{M_u^{1/n_u}} s + 1} \right)^{n_u} \tag{19}$$

In particular, for the performance weighting (W_p) M_p is the high frequency gain, A_p the low frequency gain and ω_b the crossover frequency. For the control effort weight, (W_u) τ determines the crossover frequency, A_u is the low frequency gain and M_u is the high frequency gain. Both n_p and n_u control the roll-off rates of the filters taken as 1 in this case. The shape of the filters is shown in Fig. 4 which is typical in the H_∞ framework. Note that the controller output is fixed, as it is only the applied voltage to the MAGLEV system, however the controllers inputs vary based upon the sensors utilised. i.e. SISO controller for 1 sensor, MISO controller for more sensor combinations. In fact, the order of the controller is fixed to the order of the plant and the order of the filters (currently $3 + 2 = 5^{th}$ order in a state space description - note that further controller reduction could be followed if required).

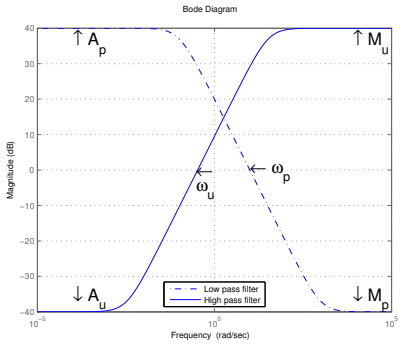

Fig. 4. Weights shape for H_∞ controller design.

C. NSGAII implementation

In this section only the necessary information is given and for more details refer to [3], [4]. The parameters used are shown in table III. The crossover probability is generally selected to be large in order to have a good mixing of genetic material. The mutation probability is defined as $1/n_v$, where n_v is the number of variables. This is appropriate in order to give a mutation probability that mutates an average of one parameter from each individual. For the simulated binary crossover parameter (SBX) and the mutations parameter it was decided to use the default value of 10 and 50 since they provide good distribution of solutions for the algorithm operations. To achieve the required constraints, different ways exist in genetic algorithms [1]. The penalty function approach [3] is used to achieve the constraint within limits. The constraint violation for each constraint, k^i, defined in Table II, is given as

$$\omega_j(k^j) = \begin{cases} |g_j(k^j)|, & if \quad g_j(k^j) < 0 \\ 0 & otherwise \end{cases} \tag{20}$$

TABLE III
NSGA-II PARAMETERS USED FOR THE EVOLUTION PROCEDURE.

Parameter	setting
Crossover probability	0.9
Mutation probability	$1/n_u$
SBX parameter	10
Mutation parameter	50
Rigid bounds	1(yes)
Population	50
Generations	100

Each soft constraint is normalised as in (21) for values less than the predefined level.

$$g_j = -\frac{k^j}{k^j_{des}} + 1 \geq 0 \tag{21}$$

Where, k^j_{des} is the predefined constraint value and k^j is the measured value. The hard constraint violation is given as

$$\psi_i(f^i) = \{^{0,}_{|h_i(f^i)|} \quad ^{if \quad h_i(f^i)=0}_{otherwise} \tag{22}$$

This is transformed into a soft constraint, allowing a small tolerance value ϵ. Therefore, the steady state error for the air gap is given as shown in (23).

$$h_i = \mid f^i \mid -\epsilon < 0 \tag{23}$$

Where f^i is the steady state error of the control effort that eventually controls the steady state error for the air gap.
The overall constraint violation is given in (24). The overall constraint violation is going to be used as a metric for the controllers that either satisfy or not satisfy the aforementioned constraints.

$$\Omega(k^{(j)}, f^{(i)}) = \sum_{j=1}^{j} \omega_j(k^{(i)}) + \sum_{i=1}^{i} \psi_i(f^{(i)}) \tag{24}$$

This constraint violation is then added to each of the objective functions values

$$\Phi_m = \phi_m + R_m \Omega(k^{(i)}, f^{(i)}) \tag{25}$$

where R_m is the penalty parameter and Φ_m the objective function value. In this case, a dynamically updated penalty parameter is required. This is useful, in order to avoid infeasible solutions and the penalty parameter is set to be a function of the generation number [10]. The penalty parameters are finalised as follows:

$$R_{i_{rms}} = C * 1, \quad R_{\ddot{z}_{rms}} = C * 0.5, \quad R_{\gamma_{opt}} = C * 1 \tag{26}$$

With, C being the generation number for the current sensor set.

IV. SIMULATIONS AND DATA ANALYSIS

The flow chart for the sensor optimisation framework, is shown in Fig. 5. The flowchart shows how the NSGAII is merged to the sensor selection framework efficiently, producing the Pareto front of optimised controllers for each possible sensor set with the required criteria. Initially, the NSGAII parameters and controller selection criteria are given. Then the first sensor set is selected and the evolutionary algorithm tunes the weights to recover the Pareto front of optimised controllers (which is equal to the number of population). After that, the controllers that satisfy all constraints are selected base on the overall constraint violation function (24). Moreover, the optimised controllers that actually satisfy the selection criteria are saved and the procedure continues with the next sensors set (if exists). The overall algorithm was tested using a Pentium 4, Dual core processor running at 2GHz with 4GB DDR memory and without the Java tool of MATLAB 7.2. The average simulation time per sensor set was about one hour and the procedure for all possible sensor sets takes about 37hours with noise-free measurements. From the simulations it can be seen that the proposed systematic framework is able to find controllers that satisfy the constraints for 29 out of 31 sensor set combinations. No controllers where found to

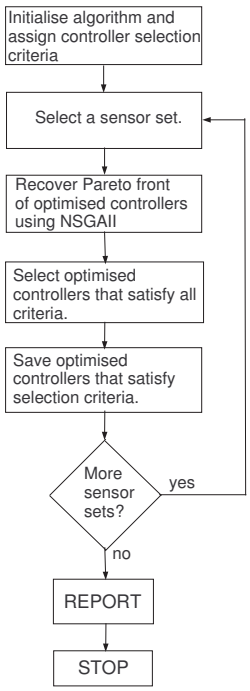

Fig. 5. Sensor selection flow chart.

meet some of the constraints ($(t_s, (z_t - z)_{e_{ss}})$) for two single sensor sets (i (current) and $(z_t - z)$ (air gap)). In particular, for a population of 50 the final result is about 1550 optimised controllers assuming none of them violates the constraints for all sensor sets. However, about 1440 optimised controllers satisfy the constraints for the 31 sensor sets.
The next step is to analyse the results based on the controller selection criteria in (27). There are no optimised controllers to satisfy the criteria with 12 out of 31 sensor sets including the full sensor set. Table IV presents the results obtained with some randomly selected sensor sets.

$$\gamma < 1 \quad and \quad \ddot{z} < 0.4m/s^2 \tag{27}$$

Ω and Ω_{noise} columns indicates if there are optimised controllers that satisfy the contraints for the corresponding sensor set based on overall constraint violation in (24). Ω_{noise} is for

noise and Ω for noise-free measurements. 'x' symbol is shown when there is no controller that satisfy the contraints and '$\surd$' is shown when there exist a number of controllers that satisfy the constraints. $n[K(s)]$ and $n[K(s)_{noise}]$ is the number of

TABLE IV
SENSOR COMBINATIONS WITH CONSTRAINTS.

id	Sensor set	noise-free		with noise	
		Ω	$n[K(s)]$	Ω_{noise}	$n[K(s)_{noise}]$
1	i	x	0	x	0
2	b	$\surd$	6	$\surd$	0
3	$(z_t - z)$	x	0	$\surd$	0
4	$\dot{z}$	$\surd$	11	x	0
5	$\ddot{z}$	$\surd$	4	$\surd$	0
6	i,$\ddot{z}$	$\surd$	17	$\surd$	3
7	b,$(z_t - z)$	$\surd$	13	$\surd$	12
8	i,$\dot{z}$,$\ddot{z}$	$\surd$	1	$\surd$	0
9	i,b,$\dot{z}$	$\surd$	5	x	0
10	i,b,$\ddot{z}$	$\surd$	0	$\surd$	5
11	b,$(z_t - z)$,$\ddot{z}$	$\surd$	0	$\surd$	3
12	i,b,$(z_t - z)$,$\dot{z}$,$\ddot{z}$	$\surd$	0	$\surd$	0

optimised controllers found to satisfy the controller selection criteria with noise and noise-free conditions respectively for the corresponding sensor set. Optimised controllers with three (id:2,4,5) out of 5 single measurements are able to meet the contraints and selection criteria assigned. The measurement with id:4 results to a Pareto front of optimised controllers depicted in Fig. 6. From the graph, it can be seen that the vertical acceleration $(\ddot{z})$ of the suspension is limited to the constraint value of $0.5m/s^2$ as required and also a trade-off between $\ddot{z}$ (ride quality) and the RMS current (i_{rms}) exists. On the same figure, it is shown that there exist two disjoint Pareto fronts of optimised controllers which are successfully recovered from the recommended evolutionary algorithm (NSGAII). The corresponding air gap deviations

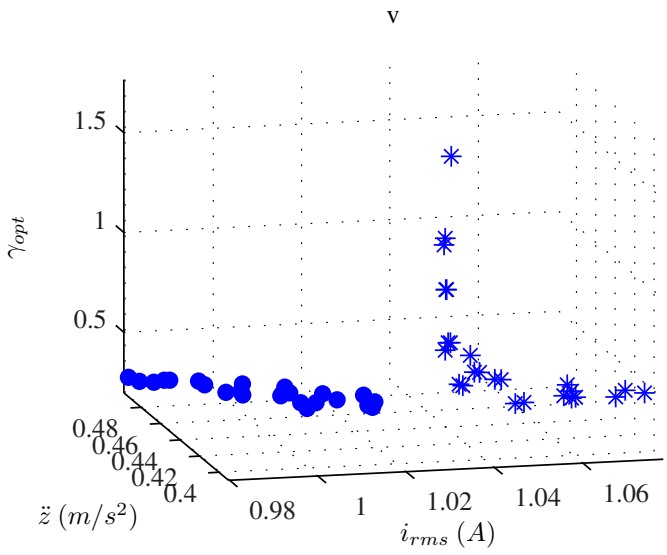

Fig. 6. Disjoint Pareto fronts with id:4 sensor set.

using id:4 sensor set are shown in Fig.7(a). It can be seen that all virtually deterministic responses remain within the constraints allowing a zero $(z_t - z)_{e_{ss}}$, a maximum of $7.5mm$ deflection and settling time less that the required $3s$. Using the id:1 sensor set (see Fig.7(b)) some constraints are violated $(\ddot{z}_{rms}, t_s$ and $(z_t - z)_{e_{ss}})$ therefore, all controllers are rejected (see Ω function). However, the suspension still remains stable

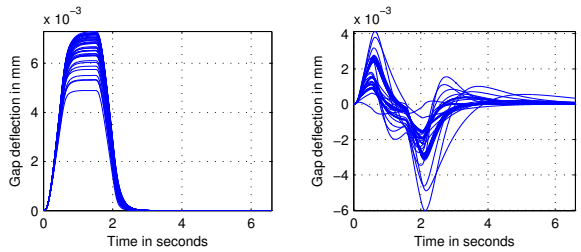

(a) *Air gap deflections with id:4 sensor set.* **(b) *Air gap deflections with id:1 sensor set.***

Fig. 7. Air gap deflection with single measurements.

with id:1 sensor set and therefore the data could be used to be part of a fault tolerant control scheme that is able to predict the behavior of the suspension. In case of faulty sensors, if the system remains with only id:1 sensor set this can lead to poor performance until the MAGLEV vehicle stops.
The Pareto front of optimised controllers with full sensor set combination (id:12) is shown in Fig.8. As it can be noted, all values of γ_{opt} are greater than the required criteria of $\gamma_{opt} < 1$ which explains why all controllers are rejected. The air gap deflections are not shown here because they look similar to the corresponding (id:4) as in Fig.7(a). Another useful remark

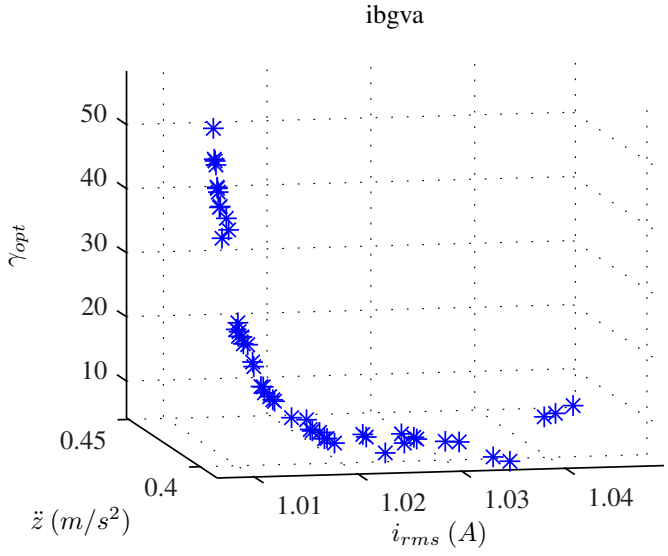

Fig. 8. Pareto front with full sensor set.

is that the control effort is limited to about 50V for the three, id:2,4,12. For the id:2 and id:12 the control effort signal is shown in Fig.9 but the control effort for the id:4 is not shown because it is similar to id:2.

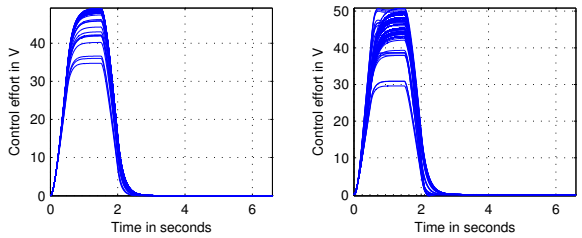

(a) *Control effort with id:12 sensor set.* **(b) *Control effort with id:2 sensor set.***

Fig. 9. Control effort with id:2 and id:12 sensor sets combinations.

A. Sensor optimisation with noisy measurements

In this section, the measurement noise is taken into account, although a similar procedure is followed as in the previous case with noise-free measurements. The difference is adding extra constraint relating to the noise issues. In fact, a simple control analysis shows that the outputs in the closed loop will not be affected much by noise. However, the control input can be quite sensitive to the noise and care should be taken to limit this. Thus the measurement noise is treated separately and the effect of the noise on the control effort is limited to $u_{noise} = 2V_{rms}$ (an extra constraint is added) and u_{noise} is introduced in the algorithm as a fourth objective ($\phi_4 = u_{noise}$) as well. The population is set to 50 and the maximum generations 200. The noise covariance for the simulations is set as 1% of the peak value from each measurement and this is updated dynamically because the peak value varies for each simulation. The optimisation for each sensor set takes about 3.5hours and the overall time taken is 105 hours on the same computer. The systematic framework presented found controllers that satisfy the assigned constraints for 24 out of 31 sensor sets.

The results shows that there exist controllers for 8 sensor sets that satisfy all constraints and the controller selection criteria shown in (27). Table IV present the results obtained with these criteria compared with the results with noise-free measurements. Column Ω_{noise} shows the constraint violations for the corresponding sensor sets and $n[K(s)_{noise}]$ is the number of controllers found to meet the controller selection criteria for noisy measurements situation. Compared to the noise-free results it can be seen that the measured noise has a significant effect on the optimisation procedure as many of the controllers for each sensor set are rejected due to noise amplification by controller.

More details follows to analyse the results. Three out of five single measurements are able to meet the constraints. The three measurements are: id:3, id:2 and id:5. It appears that, without measurement noise, only the id:1 and id:3 do not satisfy the constraints. The problem here, is that id:3 should have had solutions for the noise-free situation as well but it seems that the algorithm wasn't able to find the solution area. This could be either not sufficient chromosome population or not sufficient maximum generation. It indicates how important is to properly assign parameters for the NSGAII. Probably, for the measurement noise case the extra objective and constraint 'guide' the search space to the solution area.

The graph depicted in Fig. 10 shows the trade-off between the objectives assigned using id:5 sensor set. Clearly, there is a conflict between the objectives assigned to the problem (note that the coordinate values are normalised to unity).

The air gap deviations for the sensor set id:5 is shown in Fig. 11(a) and is compared with the air gap deviations for the full sensor set (id:12) that appears to be satisfactory in both cases. The peak values remains less that $7.5mm$ as required and the settling time less than $3s$. Note here, that the measurement noise affects the air gap deflections with the full sensor set (id:12). A sample of the control effort is shown in Fig. 12. It is clear that with the current systematic framework the noise amplitude which appears on the control effort is limited to the constrained for both sensor sets id:5 and id:12.

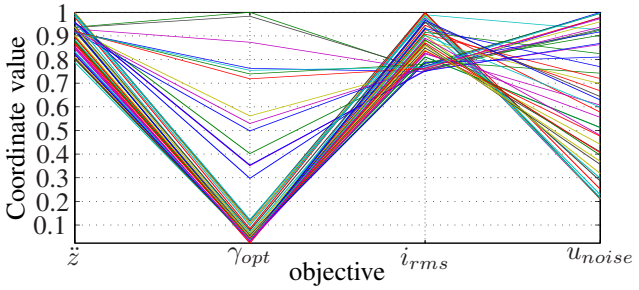

Fig. 10. Parallel cord show the trade-off between objectives with single measurement (id:5).

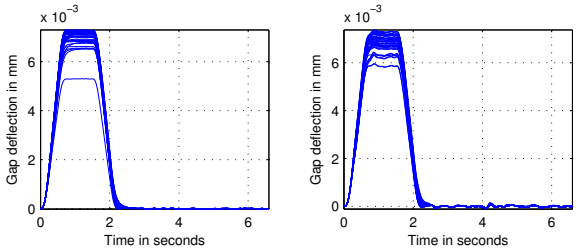

(a) *With $\ddot{z}$ measurement.* **(b) *With full sensor set.***

Fig. 11. Air gap deflections for two sensor sets.

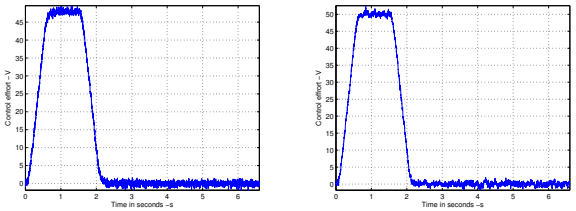

(a) *With id:5 sensor set.* **(b) *With full sensor set (id:12).***

Fig. 12. Limited noise that appears on the control effort with id:5 and id:12.

V. Conclusions and Future Work

In this paper, a systematic framework via H_∞ control design for selecting the desired sensor set that satisfies a number of constraints and controller selection criteria for a MAGLEV suspension is presented. The problem is rather

complicated to solve manually (especially tuning the weights manually for each sensor set combination), while the powerful optimisation tool based on evolutionary algorithms NSGAII is incorporated to offer faster solutions. It was found that 29 out of 31 optimised sensor configurations are tuned and perform satisfactory. The results show a variety of optimised controllers (about 1440) which can be used and the choice depends on the user's controller selection criteria. A number of useful outcomes can be seen from using the framework: The overall control system complexity and cost is reduced, or a single measurement can be used to control the suspension. Subsequently, fault probabilities are reduced. This proposed method could be used as part of a fault tolerant controller scheme, i.e using a bank of selected optimised controllers and replacing relevant controllers with other sets depending on sensor faults.

REFERENCES

[1] Coello C.A.C. Theoretical and numerical constraint-handling techniques used with evolutionary algorithms: A survey of the state of the art. *Computer Methods in Applied Mechanics and Engineering*, 191(11-12):1245–1287, 2002. Compilation and indexing terms, Copyright 2007 Elsevier Inc. All rights reserved.

[2] N. V. Dakev, J. F. Whidborne, A. J. Chipperfield, and P. J. Flemings. Evolutionary h infinity design of an electromagnetic suspension control system for a maglev vehicle. *Proceedings of the Institution of Mechanical Engineers.Part I, Journal of Systems & Control Engineering*, 211(5):345–355, 1997. Compilation and indexing terms, Copyright 2007 Elsevier Inc. All rights reserved.

[3] Kalyanmoy Deb. *Multi-objective Optimization using Evolutionary Algorithms*. John Wiley & sons Ltd, 2001.

[4] Kalyanmoy Deb, Amrit Pratap, Sameer Agarwal, and T. Meyarivan. A fast and elitist multiobjective genetic algorithm: Nsga-ii. *IEEE Transactions on Evolutionary Computation*, 6(2):182–197, 2002. Compilation and indexing terms, Copyright 2007 Elsevier Inc. All rights reserved.

[5] J. Dreo, P. Siarry, A. Petrowski, and E. Taillard. *Metaheuritics for Hard Optimization*. Springer-Verlg Berlin Heidelberg, New York, 2006.

[6] P. J. Fleming and R. C. Purshouse. Evolutionary algorithms in control systems engineering: A survey. *Control Engineering Practice*, 10(11):1223–1241, 2002. Compilation and indexing terms, Copyright 2006 Elsevier Inc. All rights reserved.

[7] R. M. Goodall. Dynamic characteristics in the design of maglev suspensions. *Proceedings of the Institution of Mechanical Engineers, Part F: Journal of Rail and Rapid Transit*, 208(1):33–41, 1994. Compilation and indexing terms, Copyright 2007 Elsevier Inc. All rights reserved.

[8] R. M. Goodall. Dynamics and control requirements for ems maglev suspensions. In *Proceedings on international conference on Maglev*, pages 926–934, Oct 2004.

[9] R. M. Goodall. The theory of electromagnetic levitation. *Physics in Technology*, Vol. 16(No 5):pp 207–213, Sept 1985.

[10] J. A. Joines and C. R. Houck. On the use of non-stationary penalty functions to solve nonlinear constrained optimization problems with ga's. In *Evolutionary Computation, 1994. IEEE World Congress on Computational Intelligence., Proceedings of the First IEEE Conference on*, pages 579–584 vol.2, 1994.

[11] Hyung-Woo Lee, Ki-Chan Kim, and Ju Lee. Review of maglev train technologies. *IEEE Transactions on Magnetics*, 42(7):1917–1925, 2006. Compilation and indexing terms, Copyright 2007 Elsevier Inc. All rights reserved.

[12] S. Skogestad and I. Postlethwaite. *Multivariable Feedback Control Analysis and Design*. John Wiley & Sons,Ltd, 2005.